



Electrochemical behaviour of 2-hydroxybenzophenones and related molecules

Emmie Chiyindiko^{a,1}, Ernst H.G. Langner^{a,2}, Jeanet Conradie^{a,b,*,3}

^a Department of Chemistry, University of the Free State, P.O. Box 339, Bloemfontein, 9300, South Africa

^b Department of Chemistry, UiT – The Arctic University of Norway, Tromsø N-9037, Norway

ARTICLE INFO

Keywords:

2-Hydroxybenzophenone
Reduction
Predict
Electron affinity
Electrophilicity index
Electronegativity
LUMO energy

ABSTRACT

An electrochemical study, using cyclic voltammetry of 2-hydroxybenzophenone and related molecules, containing various electron withdrawing and/or electron donating groups, is presented. The CV profiles of the various molecules show one sharp reduction and one small oxidation wave, coupled to the reduction wave. Density functional theory (DFT) calculations shed light on the transmission of charges through the molecule, due to the different substituent groups at the *ortho*, *meta* or *para* positions. Various DFT calculated energies relate linearly to the experimentally measured reduction potential. These obtained linear relationships can be used to predict the reduction potential of similar molecules.

Introduction

The 2-hydroxybenzophenone (HBP) framework (Scheme 1) is used extensively in an array of natural products and biologically functional molecules [1–3]. This moiety is an important component in the synthesis of various pharmaceuticals [4]. Molecules with 2-hydroxybenzophenone skeletons display a wide range of biological activities, such as anticancer [5,6], anti-HIV [7], antimicrobial [8], anti-inflammatory [9], antioxidant [10] and antitubulin activities [11]. HBPs are broadly used as sun-protection materials [13], valuable chemical auxiliaries [12] and as important precursors for the synthesis of chiral molecules [13–15] and fluorophores [16]. The 2-hydroxybenzophenone and related molecules in this study contain two oxygen donor atoms and are reported to have strong coordinating properties and ability to bind with transition metals such as Fe [17], Co [18] and Zn [19] in a bidentate manner, to form octahedral metal complexes.

The redox properties of a series of five 2-hydroxybenzophenone (HBP) molecules have been previously reported, showing that 2-hydroxybenzophenones containing an electron donating substituent, such as 2-hydroxy-4-methoxybenzophenone (4-OMe) or 2-hydroxy-4-octyloxybenzophenone (4-Oct), alter the experimental cathodic peak potential to a more negative potential than the unsubstituted 2-

hydroxybenzophenone molecule (HBP) [20]. On the other hand, 2-hydroxybenzophenones containing an electron withdrawing substituent, such as 2-hydroxy-5-chlorobenzophenone (5-Cl) and 2-hydroxy-5-bromobenzophenone (5-Br), shift the experimental reduction potential to a less negative potential than the unsubstituted 2-hydroxybenzophenone molecule (HBP) [20].

In this study, we present the electrochemical properties of seven additional 2-hydroxybenzophenones and related molecules (Scheme 1), some of whose electrochemical behaviour has not been previously reported. The molecules of this study were chosen to be even more electron donating (molecules 1 and 2) and more electron withdrawing (molecules 4 and 5) than those previously reported. Additionally, we were interested to determine the influence of an ester substituent group on the reduction potential of a substituted 2-hydroxybenzophenone (molecule 3). An experimental electrochemical study in solvent DMSO of the unsubstituted 2-hydroxybenzophenone (8) (for comparison), as well as related molecules 2-amino-5-chlorobenzophenone (11) (previously reported in DMF [21]) and 4-hydroxybenzophenone (12), has also been included, in order to investigate the influence of the type of *ortho* substituent (2-hydroxy versus 2-amino) and the position of the hydroxy substituent (2-hydroxy versus 4-hydroxy) on the reduction potential of these molecules. This experimental electrochemical study was

* Corresponding author at: Department of Chemistry, University of the Free State, P.O. Box 339, Bloemfontein, 9300, South Africa.

E-mail address: conradj@ufs.ac.za (J. Conradie).

¹ ORCID: 0000-0003-0538-3154.

² ORCID: 0000-0002-4667-3396.

³ ORCID: 0000-0002-8120-6830.

complemented by a theoretical computational chemistry study, using density functional theory (DFT) methods. Towards this end, the DFT study was extended to also include five additional 2-hydroxybenzophenone molecules, **6–10**, which have been previously reported [20,22], for a deeper understanding.

Experimental

The various 2-hydroxybenzophenone molecules were obtained from Sigma Aldrich and used without further purification.

Cyclic voltammetry

Cyclic voltammetric (CV) measurements were conducted on a BAS100B Electrochemical Analyzer linked to a personal computer, utilizing the BAS100W Version 2.3 software. Measurements were done at 293 K and temperature was kept constant to within 0.5 K. A three-electrode cell was used, with a glassy carbon working electrode (surface area 0.0707 cm²), Pt auxiliary electrode and a Ag/AgCl reference electrode (BASI P/N MF-2052). The analyte was dissolved in dimethylsulfoxide (DMSO, anhydrous, ≥99.9% Sigma Aldrich) and separated from the reference electrode with a bridge filled with a 0.1 mol dm⁻³ tetra-n-butylammoniumhexafluorophosphate (TBAHFP) in DMSO. The working electrode was polished on a Bühler polishing mat, first with 1 μm and then with ¼ micron diamond paste (in a figure-of-eight motion), rinsed with EtOH, H₂O and CH₃CN, and dried before each experiment. The electrochemistry measurements were performed on 0.002 mol dm⁻³ (or saturated) samples in DMSO, with 0.1 mol dm⁻³ tetrabutylammonium hexafluorophosphate, TBAHFP, as supporting electrolyte. The DMSO liquid was drawn from the bottle with a syringe under argon and transferred to the CV cell. The voltammograms were obtained at room temperature under a blanket of argon, to prevent traces of oxygen or moisture from entering the cell. Scan rates were varied between 0.020 and 10.240 V s⁻¹. Ferrocene was used as an internal standard, and cited potentials were referenced against the Fc/Fc⁺ couple, as suggested by IUPAC [23]. E_{pa} = anodic peak potential and i_{pa} = anodic peak current, E_{pc} = cathodic peak potential and i_{pc} = cathodic peak current. The

reduction potential is determined by the formal reduction half-wave potential $E^{0r} = (E_{pa} - E_{pc})/2$, and the peak potential separation $\Delta E_p = E_{pa} - E_{pc}$.

Density functional theory (DFT) calculations

Density functional theory (DFT) calculations were performed on the neutral ($q = 0, S = 0$), reduced ($q = -1, S = 1/2$) and oxidized ($q = 1, S = 1/2$) molecules, using the B3LYP functional which is composed of the Becke 88 exchange functional [24], in combination with the LYP correlation functional [25], as implemented in the Gaussian 16 package [26]. The triple- ζ 6-311G(d,p) basis set was used. Calculations were performed in DMSO as implicit solvent. The solvation model used is based on density (SMD) [27]. Default parameters were used for the polarizable continuum model (PCM) of the solvents. This solvation model applies the integral equation formalism variant (IEF-PCM) [28]. The input coordinates for the compounds were constructed using Chemcraft [29]. DFT energies [30–37] and molecular electrostatic potentials (MESP) [38] were calculated as described in literature [21,39].

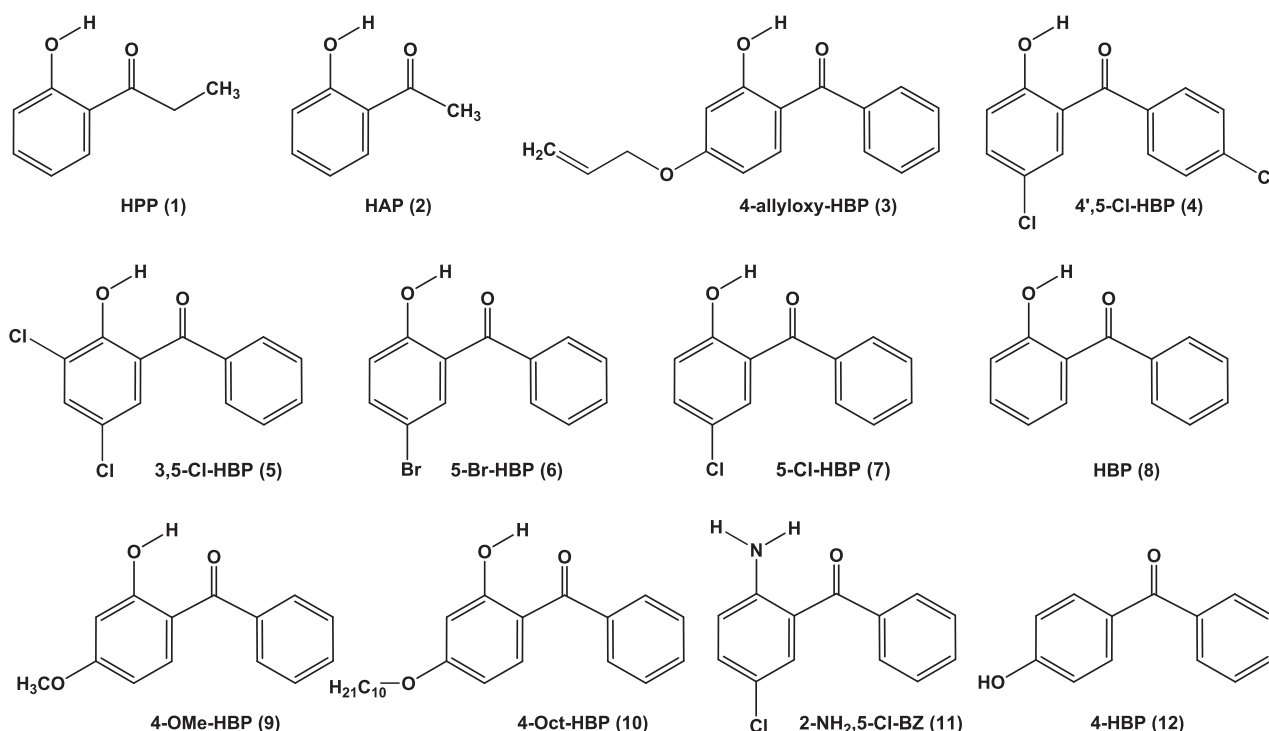
Results and discussion

DFT study

The geometries of molecules **1–12** were optimized using DFT, in order to obtain more insight into the geometry and energies involved in the reduction process of these molecules.

Geometry

In the optimized geometries of **1–2** containing only one phenyl ring, the hydroxy oxygen and carbonyl carbon are in the same plane as ring Ph1 (with dihedral angle $\Psi_1 = \text{O2C2C1C7} \approx 0$, Fig. 1). However, for molecules **3–10** containing two phenyl rings, these two phenyl groups are tilted relative to the CO group. The two dihedral angles around C7C1 and C7C1' (Ψ_1 and Ψ_2 in Fig. 1) are 10.9° and 42.2° respectively, in the neutral unsubstituted HBP molecule **8**, see Table 1. In all neutral molecules **3–10**, Ph2 is more tilted than Ph1. In molecules **3, 9** and **10**,



Scheme 1. Structure of molecules of this study, including abbreviations used for the twelve 2-hydroxybenzophenone and related molecules.

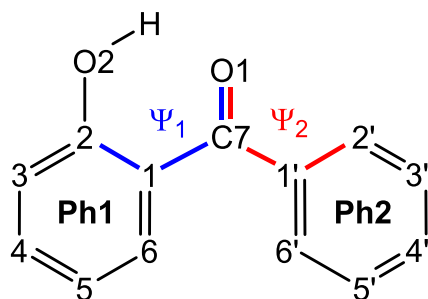


Fig. 1. (a) General structure of 2-hydroxybenzophenone, indicating the atom numbering, and the dihedral angles Ψ_1 and Ψ_2 corresponding to the tilting of phenyl rings Ph1 and Ph2 (respectively), relative to the carbonyl group.

containing electron donating alkoxy substituents, Ψ_1 is slightly smaller than in molecule **8** (9° versus 11°), while in molecules **4–7**, containing electron withdrawing halogen substituents, Ψ_1 is slightly larger than in molecule **8** (12° versus 11°). Upon reduction, both dihedral Ψ_2 and θ (the angle between the plane through Ph1 and the plane through Ph2) are decreasing, see values in Table 1. For example, θ decreases from 52.3° in neutral HBP **8**, to 35.0° in reduced **8** (Fig. 2). The decrease in dihedral Ψ_2 and angle θ upon reduction, leads to a better overlap between the rings Ph1 and Ph2, enabling a better transmission of charges between Ph1 and Ph2 in the reduced molecule.

Both molecules **7** and **11** have a Cl in the *meta* position, while **7** has a hydroxy and **11** an amino substituent in the *para* position. In both **7** and **11** a hydrogen bond is formed to the carbonyl oxygen from the hydroxy (in **7**) or from an amino hydrogen (in **11**), although dihedral Ψ_1 is much larger in both neutral and reduced **11** than in neutral and reduced **7**. However, the angle θ in neutral **7** is 51.9° (and 35.5° in reduced **7**), while angle θ in neutral **11** is 56.8° (and 45.8° in reduced **11**). There

should thus be a better transmission of charges between Ph1 and Ph2 in both neutral and reduced **7** with smaller angle θ , than in neutral and reduced **11** with larger angle θ . This could contribute to a more positive reduction potential for **7** compared to **11** [40], as was indeed experimentally observed; see the CV section below.

Similarly, when comparing the geometries of unsubstituted 2-hydroxybenzophenone (**8**) and 4-hydroxybenzophenone (**11**), the angle θ in neutral **8** is 52.3° (and 35.0° in reduced **8**), while angle θ in neutral **11** is 55.8° (and 39.6° in reduced **11**). There should thus be a better transmission of charges between Ph1 and Ph2 in both neutral and reduced **8** than in neutral and reduced **11**. This could contribute to a more positive reduction potential for **8** compared to **11** [40], as is indeed experimentally observed; see CV section below.

The amount of flow of electron density between rings Ph1 and Ph2, due to better overlap between Ph1 and Ph2 in molecules **3–12**, is a consequence of either the electron donating or withdrawing properties of the substituents on Ph1 and Ph2. This is indeed experimentally observed in the various reduction potentials, measured experimentally for molecules **3–12** in the electrochemistry (CV) section.

Frontier MOs

Reduction occurs when the potential applied to the electrochemical cell containing a chemical species in solution, is enough to move an electron from the working electrode into the lowest unoccupied molecular orbital (LUMO) of the species. The HOMOs (highest occupied molecular orbitals) and LUMOs of 2-hydroxybenzophenones and related molecules **1–5**, **8**, **11** and **12**, are shown in Fig. 3 (HOMOs and LUMOs of **6–7** and **9–10** are similar [20]). The HOMO of the neutral molecules is predominantly located on the hydroxy-substituted phenyl ring Ph1. The LUMO is mainly located on the carbonyl moiety, but is also distributed over the phenyl rings of the molecule. Reduction in molecules **1–12** will therefore occur mainly on the CO group, while the added electron will spread out over the phenyl groups of the reduced

Table 1

The B3LYP/6–311+G(2df,2p) calculated angles θ (angle between the plane through Ph1 and the plane through Ph2), and dihedral angles Ψ_1 and Ψ_2 (see Fig. 1 for definition of dihedrals), in **1–12**.

No	Hydroxybenzophenone	Neutral complex			Reduced anion		
		Ψ_1	Ψ_2	θ	Ψ_1	Ψ_2	θ
1	HPP	0.0	–	–	1.9	–	–
2	HAP	0.0	–	–	0.0	–	–
3	4-allyloxy-HBP	8.7	44.0	52.5	17.2	16.3	33.9
4	4',5'-Cl-HBP	12.0	40.7	51.6	15.7	18.9	34.9
5	3,5'-Cl-HBP	12.1	40.7	51.7	11.8	24.7	36.8
6	5-Br-HBP	11.5	41.4	52.0	14.1	21.5	35.8
7	5-Cl-HBP	11.8	41.3	51.9	14.3	20.9	35.5
8	HBP	10.9	42.2	52.3	16.0	18.8	35.0
9	4-OMe-HBP	8.6	44.4	52.8	17.2	16.0	33.5
10	4-Oct-HBP	8.6	44.3	52.7	17.1	16.4	33.9
11	2-NH ₂ ,5-Cl-BZ	15.4	42.9	56.8	32.1	12.8	45.8
12	4-HBP	23.8	34.0	55.8	23.0	14.8	39.6

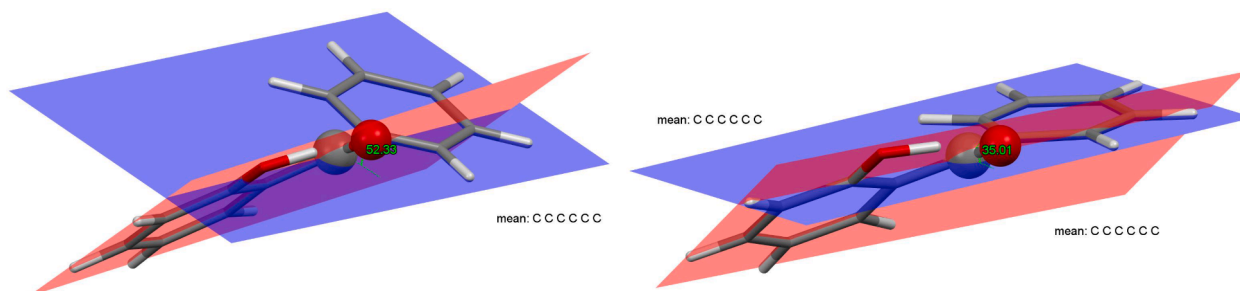


Fig. 2. The B3LYP/6–311+G(2df,2p) optimized geometries of neutral (left) and reduced (right) unsubstituted HBP **8**, showing the planes through Ph1 (red) and Ph2 (blue), with the angle θ between the planes (indicated in green). Colour code of the atoms (online version): C (black), O (red), H (grey), with the carbonyl C and O atoms shown as balls.

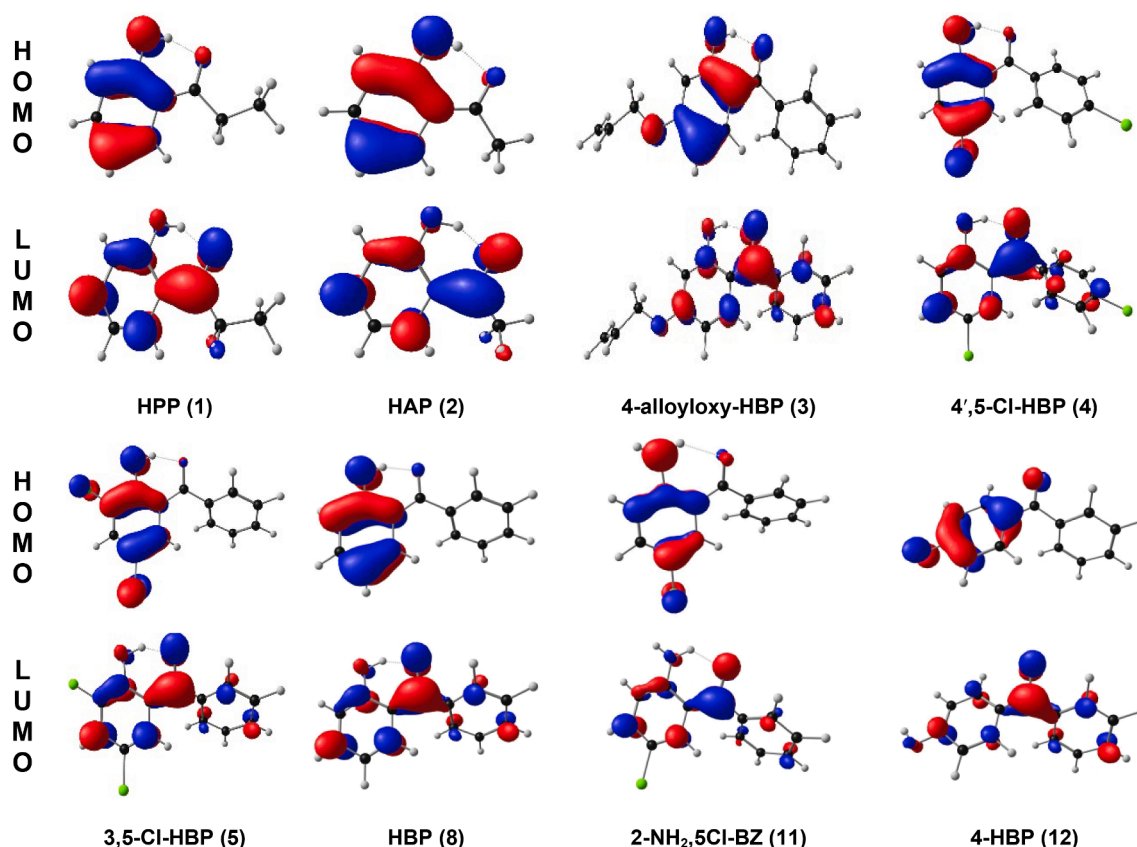


Fig. 3. B3LYP/6-311+G(2df,2p) calculated HOMOs and LUMOs of the indicated neutral 2-hydroxybenzophenones and related molecules. A contour of $0.06 \text{ e}/\text{\AA}^3$ was used for the MO plots. Colour code of the atoms (online version): Br (red), Cl (green), N (blue), C (black), O (red), H (grey).

molecule to form a radical anion.

Electron distribution

The calculated spin density of the reduced anion gives an indication of the charge distribution of the unpaired electron added upon reduction, resulting in the radical species. Calculated spin density can be

visualized by a spin density plots (Fig. 4) and quantized by Mulliken spin populations on the different atoms (Table 2). Distribution of the Mulliken spin population of the reduced anions of these 2-hydroxybenzophenones and related molecules 1 – 12, is indicated by the ratio [Ph1: CO: Ph2], shown in Fig. 4 and tabulated in Table 2 (Ph1 and Ph2 are defined in Fig. 1) The added electron upon reduction is mainly located

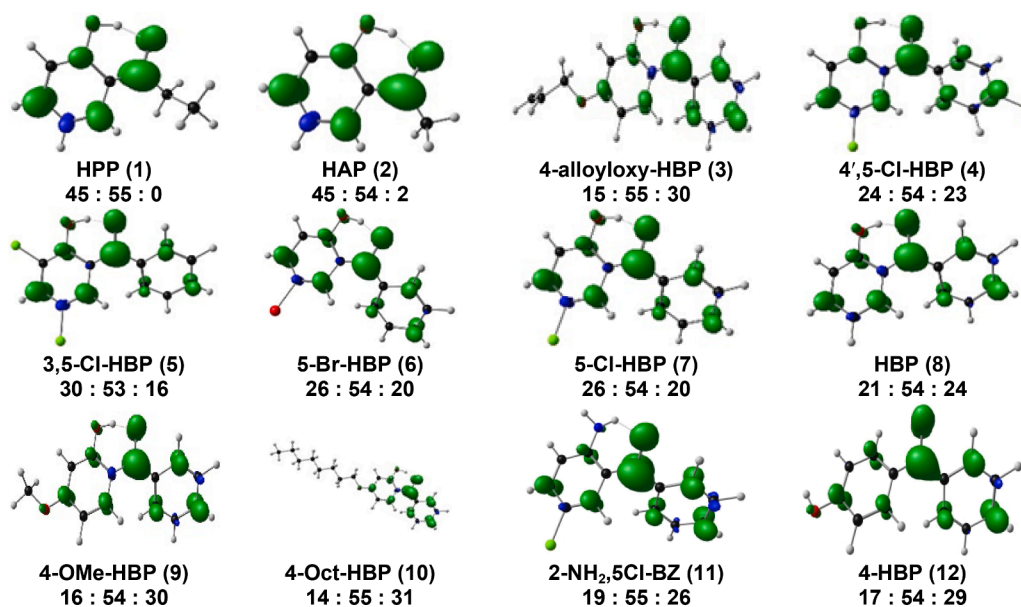


Fig. 4. B3LYP/6-311+G(2df,2p) calculated spin density plots of the twelve indicated reduced molecules, the anions of 1–12. The Mulliken spin density distribution is indicated by the % ratio [Ph1: CO: Ph2] below each molecule, where Ph1 is the phenyl ring containing the hydroxy group. A contour of $0.006 \text{ e}/\text{\AA}^3$ was used for the spin plots. Colour code of the atoms (online version): Br (red), Cl (green), N (blue), C (black), O (red), H (grey).

Table 2

Mulliken spin distribution indicated by the ratio [Ph1: CO: Ph2], of the indicated substituted 2-hydroxybenzophenones and related molecules 1 – 12 from this study.

No	Molecule	Mulliken Spin Density %		
		Ph1	CO	Ph2
1	HPP	44.7	55.3	0.0
2	HAP	44.8	53.5	1.7
3	4-alloxy-HBP	15.3	54.6	30.2
4	4',5'-Cl-HBP	23.6	53.5	22.9
5	3,5'-Cl-HBP	30.4	53.3	16.3
6	5-Br-HBP	26.3	53.8	19.9
7	5-Cl-HBP	25.8	54.1	20.1
8	HBP	21.5	54.2	24.4
9	4-OMe-HBP	15.5	54.3	30.2
10	4-Oct-HBP	14.3	55.2	30.5
11	2-NH ₂ ,5-Cl-BZ	19.0	55.1	25.9
12	4-HBP	16.9	54.1	29.0

on the carbonyl group moiety *ca.* 54%. Reduction thus largely occurs on the CO group, and spread out over the rest of the molecule, resulting in an unstable radical species. Electron density largely varies in phenyl rings Ph1 and Ph2 for reduced 3 – 12, depending on the substituent groups attached to the Ph1 and Ph2. For the unsubstituted 2-hydroxybenzophenone **8**, the spin density is approximately evenly distributed in Ph1 and Ph2.

Due to electronic influences, it is generally observed that electron withdrawing substituent groups (e.g. **5** (3,5-Cl)) on one phenyl ring, generally withdraws the electron density towards the phenyl ring it is attached to (Ph1), while an electron donating substituent groups (e.g. **3** (4-alloxy)) on one phenyl ring, generally shift the electron density towards the other phenyl ring (Ph2). Relative to HBP, **8**, the % spin population on CO is slightly higher for molecules **3**, **9** and **10** containing electron donating substituent groups and slightly lower for molecules **4** – **7** containing electron withdrawing substituent groups, see Fig. 5 and Table 2. For molecule **4** with an electron withdrawing substituent group on each phenyl ring, the electron density is almost evenly spread out across both phenyl rings. For the reduced complexes **1** and **2**, the alkyl group donates electron density to the phenyl group, while the CO group have *ca.* 54% spin population. Thus, replacing the second phenyl ring (in 2-hydroxybenzophenone **8**) with an alkyl group (methyl or ethyl as in **1** and **2** respectively) does not change the locus of the reduction centre.

The position of the substituent on the phenyl ring relative to the

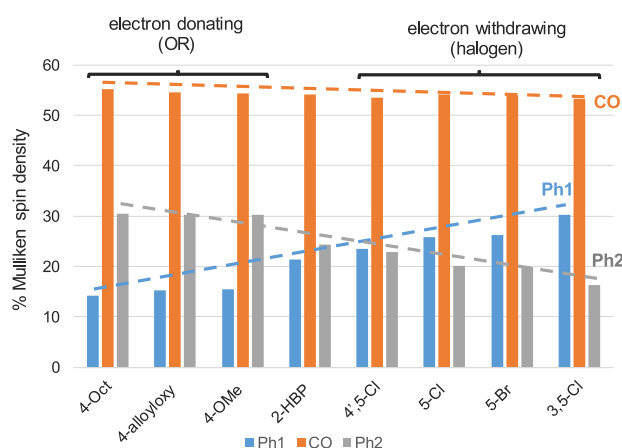


Fig. 5. B3LYP/6-311+G(2df,2p) calculated Mulliken spin population distribution of the indicated reduced anions of molecules 3 – 10. The Mulliken spin density distribution is indicated by the % on Ph1 (blue), on CO (orange) and on Ph2 (gray) on the vertical axis. (For interpretation of the references to colour in this figure legend, the reader is referred to the web version of this article.)

reduction centre CO in molecules **3** – **10**, influences the electronic effect on any substituent on the phenyl rings. Inductive electronic contributions that arise due to electronegativity differences, can occur from *ortho*, *meta* and *para* substituents, while alkoxy groups on the *ortho* and *para* positions also donate electron density through resonance [41]. The larger amount of spin density on the Ph2 (*ca.* 30%) of reduced molecules **3**, **9** and **10**, thus results from a combination through induction and the lone pair electron density donation through resonance of electron-donating alkoxy groups (OR). However, Ph2 becomes increasingly deficient of the unpaired electron density as Cl and Br substituents on Ph1-substituents withdraws electron density to Ph1 through induction. Molecule **5** containing two halide groups have 30.4% spin density on Ph1, while molecules **6** and **7** with one halide group has on average 26% on Ph1.

Molecules **8** and **12**, have a hydroxy substituent in the *ortho* and *para* positions respectively. The OH group donates electron density through resonance and through induction at the *ortho* and *para* positions. The electronic inductive effect of a substituent in the *ortho* position is found to be much larger than its effect in the *para* position [42], but steric effects plays a role for *ortho* substituents, complicating direct comparison of the electronic effect of an *ortho* versus *para* substituent. However, OH in molecule **12** (4-HBP) donates more electron density to Ph2 than molecule **8** (HBP), 29.0% in **12** versus 24.4% in **8**, suggesting that the *para* OH group in **12** is more electron donating than the *ortho* OH group in **8**. This may lead to a more negative reduction potential for **12** than for **8**, as indeed experimentally observed, see CV section below.

Molecules **7** and **11** have a Cl in the *meta* position while **7** has a hydroxy and **11** an amino substituent in *para* position. In both **7** and **11** a hydrogen bond is formed to the carbonyl oxygen from the hydroxy or an amino hydrogen. The amino group in **11** donates more electron density to Ph2 than molecule **7**, 25.9% in **11** versus 20.1% in **7**, suggesting that the *para* NH₂ group in **11** is more electron donating than the *para* OH group in **7**. This may lead to a more negative reduction potential for **11** than for **7**, as indeed experimentally observed, see CV section below.

These shifts in electron density are theoretically visualized by the spin density plots (Fig. 4) and experimentally reflected by the different reduction potentials reported in the electrochemistry (CV) section.

CV study

Experimental study

The electrochemical properties of molecules **1** – **5**, **8**, **11** and **12**, described in Scheme 1, were examined using cyclic voltammetry (CV) measurements in DMSO solvent media. Cyclic voltammograms obtained for the five derivatives **1** – **5** (and unsubstituted 2-hydroxybenzophenone **8** for comparison) at a scan rate of 0.100 Vs⁻¹ are shown in Fig. 6. Further CVs with varying scan rates up to a scan rate of 10.24 Vs⁻¹ showed the same redox process as for 0.100 Vs⁻¹. The values obtained for the peak anodic potential (E_{pa}), peak cathodic potential (E_{pc}), peak separation (ΔE_p) and the corresponding formal reduction potential (E^0 in V) at the scan rate of 0.100 Vs⁻¹, are tabulated in Table 3. The species in this study show a very sharp reduction peak, with a very small re-oxidation peak coupled to the reduction peak, which become more pronounced at higher scan rates (Fig. 7). The re-oxidation peak increases with scan rate, implying that the reduced radical that formed upon reduction is relatively stable at higher scan rates on the timescale of the CV experiment. The locus of the added electron upon reduction, which is mainly located on the carbonyl group, is described in the previous section; see also Figs. 3 & 4 and Table 2.

The peak cathodic current follows the Randles-Ševčík equation, indicating that the reduction process is diffusion-controlled [43]; see Fig. 7 for unsubstituted molecule HBP (**8**) and substituted 3,5-Cl-HBP (**5**) as examples. However, the peak current ratios i_{pa}/i_{pc} are much lower than 1, indicating that the reduced radical that forms upon reduction, is unstable and partially decomposes before re-oxidation occurs. The peak separation lies between $\Delta E_p = 0.072 - 0.095$ V for the 0.100 Vs⁻¹ scans,

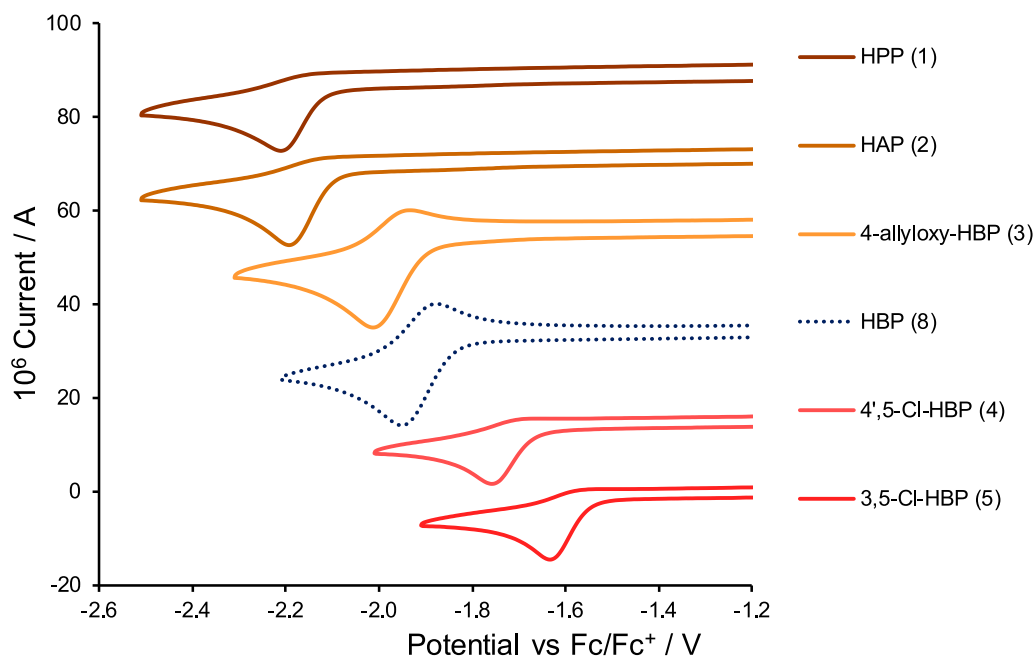


Fig. 6. Cyclic voltammograms (versus Fc/Fc^+) of $0.002 \text{ mol dm}^{-3}$ solutions of 2-hydroxybenzophenone (HBP) molecules 1–5 (and unsubstituted 2-hydroxybenzophenone (8) for comparison) in DMSO, at 0.100 Vs^{-1} scan rate.

Table 3

Data for the experimental reduction potentials ($\text{V vs Fc}/\text{Fc}^+$), obtained from *ca.* $0.002 \text{ mol dm}^{-3}$ DMSO solutions of molecules 1 – 12, listed at scan rate 0.100 Vs^{-1} as obtained in this study, as well as calculated DFT energies (in eV) and redox potential ($\text{V vs Fc}/\text{Fc}^+$).

		Experimental				Calculated							
		E_{pc}	E_{pa}	$E^{\text{O}^{\bullet}}$	ΔE	EA	IP	E_{LUMO}	χ	μ	η	ω	E_{calc}
1	HPP ^a	-2.210				2.47	6.38	-2.08	4.43	-4.43	3.91	2.50	-2.518
2	HAP ^a	-2.193				2.49	6.40	-2.13	4.45	-4.45	3.92	2.52	-2.498
3	4-allyloxy-HBP	-2.017	-1.934	-1.976	0.083	2.64	6.25	-2.18	4.44	-4.44	3.61	2.73	-2.359
4	4',5-Cl-HBP ^a	-1.757				2.99	6.35	-2.59	4.67	-4.67	3.36	3.24	-1.997
5	3,5-Cl-HBP ^a	-1.633				3.04	6.40	-2.67	4.72	-4.72	3.35	3.32	-1.940
6	5-Br-HBP ^b	-1.851	-1.779	-1.815	0.072	2.92	6.32	-2.53	4.62	-4.62	3.40	3.14	-2.068
7	5-Cl-HBP ^b	-1.886	-1.804	-1.845	0.082	2.91	6.33	-2.53	4.62	-4.62	3.42	3.12	-2.073
8	HBP	-1.953	-1.876	-1.915	0.077	2.78	6.39	-2.38	4.59	-4.59	3.61	2.91	-2.204
9	4-OMe-HBP ^b	-2.019	-1.947	-1.983	0.072	2.63	6.25	-2.17	4.44	-4.44	3.62	2.73	-2.359
10	4-Oct-HBP ^b	-2.029	-1.954	-1.992	0.075	2.62	6.23	-2.16	4.42	-4.42	3.60	2.72	-2.371
11	2-NH ₂ ,5-Cl-BZ	-2.158	-2.078	-2.118	0.080	2.63	5.73	-2.19	4.18	-4.18	3.10	2.82	-2.359
12	4-HBP	-2.138	-	-	-	2.49	6.43	-2.10	4.46	-4.46	3.94	2.52	-2.504

a Re-oxidation peak appear only at higher scan rates.

b Values from reference [20].

which is larger than the expected value of $\Delta E_{\text{p}} = 0.059 \text{ V}$ for a one electron transfer process [44]. The reduction process of the HBP derivatives 1–10 could therefore be considered quasi-reversible [45–47]. The diffusion coefficient obtained from the peak current/scan rate data shown in Fig. 7 (b), gives a diffusion coefficient for unsubstituted HBP (8) in DMSO of $1.93 \times 10^{-6} \text{ cm}^2 \text{ s}^{-1}$, which compares well with the reported value of $3.9 \times 10^{-6} \text{ cm}^2 \text{ s}^{-1}$ obtained in molten acetamide at $85 \text{ }^{\circ}\text{C}$.

The experimental reduction potential of the derivatives follows the order from most negative to least negative, in the order of molecule 1 > 2 > 10 > 3 > 9 > 8 > 7 > 6 > 4 > 5 (Table 3). Molecules with electron withdrawing groups (e.g. 4 and 5) yield more positive reduction potentials, while molecules with electron donating groups (e.g. 1 and 2) yield more negative reduction potentials in DMSO. The electron withdrawing effect of the substituent groups are cumulative; for example, molecules 4 and 5 with two Cl groups have more positive redox potentials than 7. Molecule 4 has an electron withdrawing (Cl) group on

each phenyl ring, simultaneously withdrawing electron density from each phenyl ring, while in molecule 5 both Cl groups are withdrawing electrons from only one phenyl ring, leading to a less negative reduction potential for 5 than for 4.

In Fig. 8(a) comparative CVs of 2-hydroxybenzophenone (HBP, 8) and 4-hydroxybenzophenone (12) are shown, in order to illustrate the influence of the position of the hydroxy group on the resulting redox potential. 4-Hydroxybenzophenone (12) is reduced at a more negative potential, indicating that the electronic influence in the *para* position (4-OH) due to induction and resonance, is more electron donating relative to the *ortho* position (2-OH), due to induction and resonance and steric effects in the *ortho* position. This also agrees with the finding that the electrical effect of a substituent in the *ortho* position is about 0.75 times its effect in the *para* position [42]. The reduction potential of 4-HBZ (12) with hydroxy in the *para* position, is even slightly more negative than the reduction potential of the 2-hydroxybenzophenones 3, 9 and 10 containing an alkoxy group in the *para* position. However, the reduction

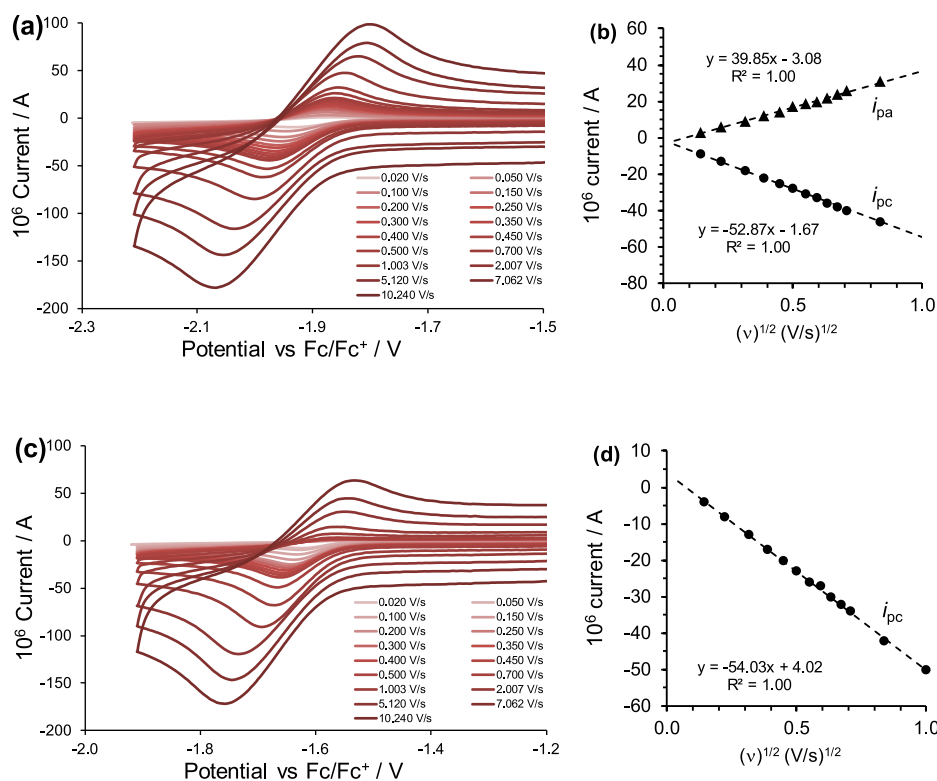


Fig. 7. CVs of molecules (a) unsubstituted HBP (8) and (c) substituted 3,5-Cl-HBP (5) in DMSO, at scan rates varying from 0.020 (smallest peak current) – 10.240 V s⁻¹ (largest peak current). Linear relationships are plotted between the peak current (i_p) of the reduction peak of molecules for (b) HBP (8) and (d) 3,5-Cl-HBP (5) in DMSO, versus the square root of the scan rate (v^{1/2} in (V/s)^{1/2}), as predicted by the Randles–Ševčík equation.

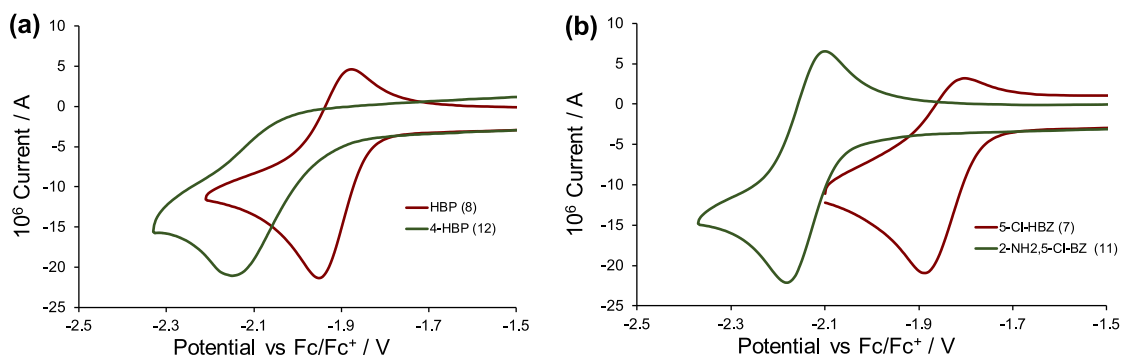


Fig. 8. Cyclic voltammograms (versus Fc/Fc⁺) of ca. 0.002 mol dm⁻³ solutions of (a) 4-hydroxybenzophenone (4-HBZ, 12) and 2-hydroxybenzophenone (HBP, 8) with hydroxy groups substituted in different positions; as well as scans of (b) 5-Cl-HBZ (7) and 2-NH₂,5-Cl-BZ (11), all in DMSO only at 0.100 V s⁻¹ scan rate.

process of 4-HBZ (12) is completely irreversible with no observed re-oxidation peak for scan rates up to 1 V s⁻¹. The added electron upon reduction in the reduced radical of molecules 3 – 10 is probably slightly better stabilized by the hydrogen bond and better overlap of Ph1 and Ph2 in reduced molecules 3 – 10, than in reduced molecule 12.

In Fig. 8(b) comparative CVs of 5-Cl-HBZ (7) and 2-NH₂,5-Cl-BZ (11) are shown together to illustrate the influence of the amino (NH₂) versus the hydroxy (OH) group in the two molecules on the resulting redox potential. The two molecules are isostructural, since both molecules have a hydrogen bond to the central carbonyl group. Amino is more electron donating than hydroxy, explaining the more negative reduction potential for 11 than for 7. At 0.100 V s⁻¹, both molecules have a similar small re-oxidation peak.

Influence of substituents

The good communication between the various substituents and the rest of the molecule in complexes 1–12 is reflected by the large shift in the experimental reduction potentials, for molecules containing electron donating versus electron withdrawing substituents. The electronic property of aromatic substituents can be expressed by the Hammett substituent constants. A linear trend between the experimental reduction potential of 3–10 and the Hammett substituent constants for the molecules (*meta* or *para* as applicable) [41] was obtained, see Fig. 9(a). A Hammett value for *ortho*-OH in molecules 3 – 10 was not added to these graphs, since the use of Hammett constants for *ortho*-substituted benzene derivatives are generally unsuccessful, due to their additional steric effects [42]. Molecules 11 and 12 are therefore also not included in this relationship, due to their *ortho* substituents not being OH.

The effect of the electronic property of substituents was also

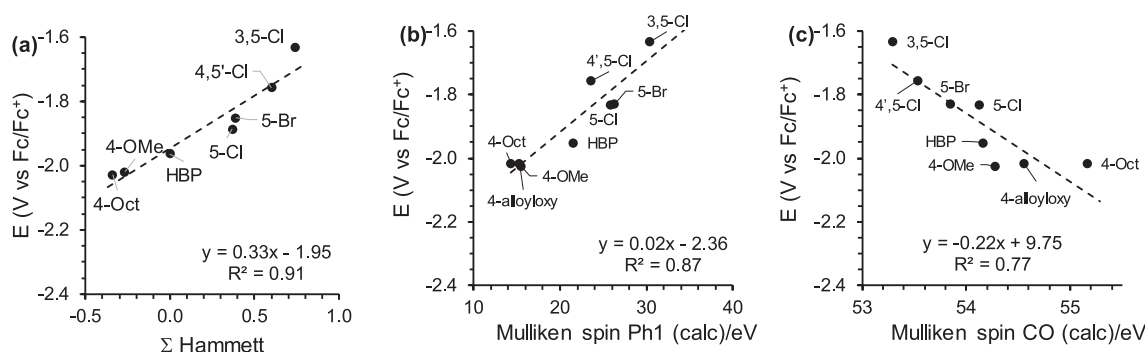


Fig. 9. The linear relationships found between the reduction potential (E_{pc}) (V versus Fc/Fc^+) of the 2-hydroxybenzophenone molecules 3–10, and (a) sum of the Hammett substituent constants of the substituent groups, (b) sum of the Mulliken spin population on Ph1 and (c) Mulliken spin population on CO. Hammett substituent constants used ($\sigma_m = 0.39$ (Br), 0.37 (Cl), 0 (H) and $\sigma_p = 0.23$ (Cl), -0.27 (OMe), -0.34 (OBu) [41]).

illustrated theoretically, by the DFT calculated Mulliken spin populations located on the CO and phenyl groups in molecules 3–10 (Fig. 4 and Table 2). A linear trend between the experimental reduction potential and the computed % Mulliken spin distribution on Ph1, CO and Ph2 (defined in Fig. 1) of molecules 3–10 was obtained; see Fig. 9(b) and (c).

Theoretical prediction of reduction potential

Computational chemistry calculated energies can be used to predict experimental redox potentials for series of related molecules, extrapolated from existing relationships between experimental reduction potential and DFT calculated energies [48–52]. Although electrochemical data for some of the molecules has been reported previously, this report is the first comprehensive study with additional 2-hydroxybenzophenones and related molecules, containing also other electron donating

or electron withdrawing groups than the molecules previously reported. Consequently the range of reduction potentials of the molecules in this study was extended from 0.2 V (previously reported for 5 molecules [20]) to 0.6 V for the twelve molecules in this study. Relationships between the experimental reduction potential of molecules 1–12 and DFT calculated solvent phase energies are shown in Fig. 10, with the corresponding data provided in Table 3. The relationships obtained hereby, lead to the following insights.

The energy of the LUMO (E_{LUMO}), which is the orbital involved in the reduction process (Fig. 10(a)), is inversely proportional to the experimental reduction potential, resulting in a graph with a negative slope. A LUMO with a lower energy is less stable, has a higher affinity for electrons and can accept an electron more easily. A molecule with a lower energy LUMO thus results in a reduced species at a more positive potential. The π -resonance system of the LUMO of the 4-alkoxyhydroxybenzophenones 3, 9, 10 and also the 4-hydroxybenzophenone 11,

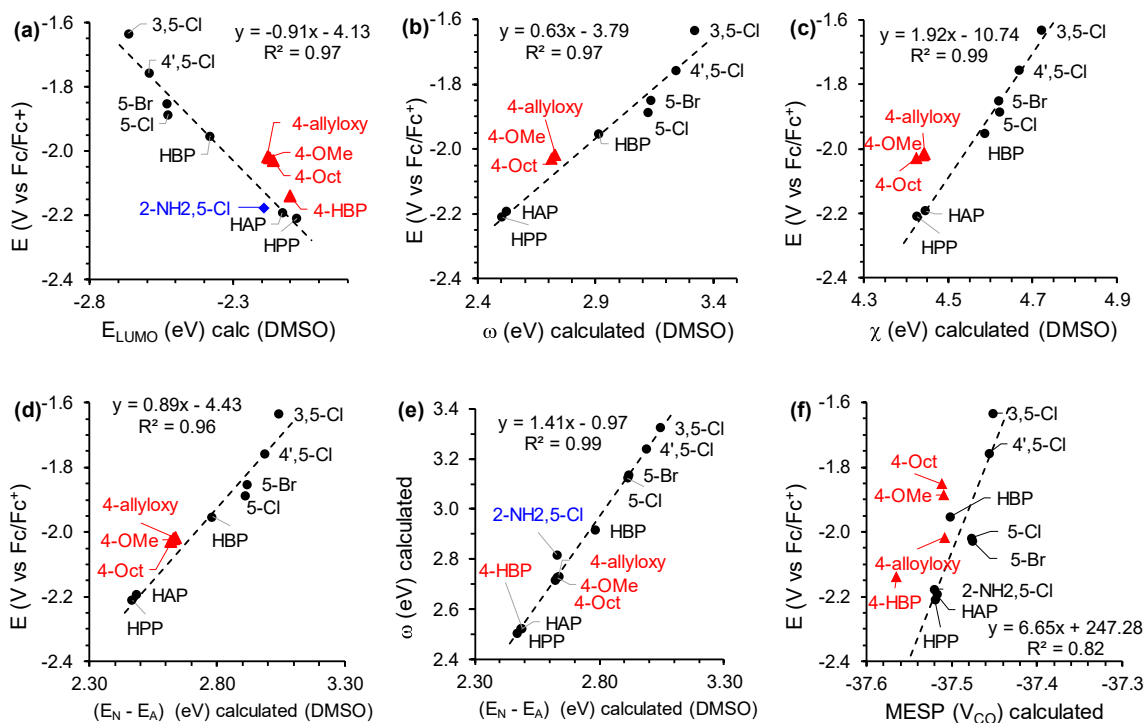


Fig. 10. Graphs of the linear relationships found between the reduction potential (E_{pc}) (V versus Fc/Fc^+) of the indicated 2-hydroxybenzophenone and related molecules, and various energies calculated by computational chemistry in the DMSO solvent phase, namely: (a) E_{LUMO} , (b) electrophilicity index (ω), (c) electronegativity (χ_R), (d) energy difference ($E_{Neutral} - E_{Anion}$), (e) the relationship between the electrophilicity index (ω) and energy difference ($E_{Neutral} - E_{Anion}$) and (f) the MESP on CO of the reduced molecule. Red triangular and blue diamond points were not considered in the linear fit. (For interpretation of the references to colour in this figure legend, the reader is referred to the web version of this article.)

extends onto the oxygen of the 4-alkoxy substituent, see the LUMOs in Fig. 3. Due to the additional resonance effect involving this 4-alkoxy and 4-hydroxy oxygen, in addition to the inductive electronic effect, these molecules **3**, **9**, **10** and **11** (marked by red triangles in Fig. 10(a)), deviate from the reduction potential $-E_{\text{LUMO}}$ trendline of the rest of the molecules. A similar result has been previously reported for redox potential relationships involving a series of benzophenone molecules, where the molecules containing aromatic rings with alkoxy substituents deviate from relationships involving molecules with alkyl substituents [21]. However, this study found that 2-hydroxybenzophenones with alkyl or halogen substituents do not deviate but follow the same linear reduction potential $-E_{\text{LUMO}}$ relationship.

Further, the experimental reduction potential of molecules **1**, **2**, **4** – **8**, also related linearly to the DFT calculated electrophilicity index (ω , measure of electrophilic power of atoms and molecules [39]), electro-negativity (χ , measure of the tendency of an atom to attract electrons) and solvent phase calculated energy difference ($E_{\text{Neutral}} - E_{\text{Anion}}$), that is similar to the electron affinity (EA, the amount of energy released when an electron is attached to a neutral atom or molecule in the gaseous state) of the molecules, as shown in Fig. 10(b)–(d) respectively. Molecule **11** with a 2-amino substituent shows a similar reduction potential $-E_{\text{LUMO}}$ trend than molecules **1**, **2**, **4** – **8**, but deviates slightly from the trends shown in Fig. 10(b)–(d). The computed adiabatic solvent phase calculated energy difference ($E_{\text{Neutral}} - E_{\text{Anion}}$) and electrophilicity index (ω) of all molecules **1** – **12** are highly correlated, as seen in Fig. 10(e), since both these properties measure the propensity of electron intake [53]. In Fig. 10(f) a general trend is observed, namely that the molecular electrostatic potential (MESP) on the CO group also decreases (more negative) as the experimental reduction potential of the molecules decrease (more negative). Thus, molecules containing electron donating groups lead to a lower MESP on CO. The MESP potential is known to be used for prediction of reduction potentials of molecules [54,55].

The linear relationships obtained from the graphs in Fig. 10 are a measure of the reliability of the results obtained in this study. Good linear correlation between experimental and calculated results is important, since these linear equations can be used to predict the reduction potential of further substituted 2-hydroxybenzophenones and structural related molecules. This capability is anticipated to be of great aid in the pre-design (before synthesis) of customized complexes with specific required redox properties, without first having to work through often costly and tedious experimental processes.

Conclusions

The reduction process of 2-hydroxybenzophenone and related molecules could be described as quasi-reversible, since the experimental peak current ratio is lower than 0.5 and the peak separation $\Delta E_p = 0.072$ – 0.095 V, for the 0.100 Vs^{-1} scans. The reduction process of 4-hydroxybenzophenone is irreversible. The experimental reduction potential values clearly show that derivatives of 2-hydroxybenzophenone containing electron withdrawing groups (e.g. Cl, Br), have more favourable reduction potentials (less negative reduction potential), while derivatives with electron donating groups (e.g. OMe, OEt), have less favourable reduction potentials (more negative reduction potential), compared to the unsubstituted 2-hydroxybenzophenone. The difference of nearly 0.6 V in reduction potential of 2-hydroxybenzophenones and related molecules with substituent groups, illustrates the sensitivity of the reduction process to the type and position of substituents on the aromatic rings, indicating that excellent communication exists between the 2-hydroxybenzophenone backbone and the various substituent groups.

The character of the DFT calculated LUMO and Mulliken spin plots of the optimized neutral as well as reduced benzophenones respectively, shows that electron donating substituent groups on one phenyl ring (Ph1) shift the electron density towards the other phenyl ring (Ph2), whereas electron withdrawing substituent groups on one ring phenyl

(Ph1) generally withdraw the electron density towards their own phenyl ring which they are attached to (Ph1). The redox potentials of 2-hydroxybenzophenones containing alkyl or halogen substituents, correlate well with their theoretically calculated LUMO energies and solvent phase calculated energy difference ($E_{\text{Neutral}} - E_{\text{Anion}}$). 2-Hydroxybenzophenone molecules with oxygen-containing groups, such as 4-alkoxy, 4-methoxy and 4-octyloxy substituted benzophenones, did not fit this relationship, due to the enhanced resonance electronic effect from the lone pair electrons on the oxygen of the *para* alkoxy substituent to the 2-hydroxybenzophenone backbone.

CRedit authorship contribution statement

Emmie Chiyindiko: Investigation, Validation, Formal analysis, Data curation, Methodology, Writing – review & editing. **Ernst H.G. Langner:** Resources, Funding acquisition, Writing – review & editing. **Jeanet Conradie:** Conceptualization, Supervision, Resources, Validation, Methodology, Funding acquisition, Project administration, Writing – review & editing.

Declaration of Competing Interest

The authors declare that they have no known competing financial interests or personal relationships that could have appeared to influence the work reported in this paper.

Acknowledgements

The authors are grateful to acknowledge the Central Research Fund of the University of the Free State, as well as the Sasol University Collaboration Programme and the National Research Foundation (NRF) of South Africa for financial support (Grant Nos: 129270 (JC) and 132504 (JC)). The High-Performance Computing facility of the UFS, the CHPC of South Africa (Grant No. CHEM0947) and the Norwegian Supercomputing Program (UNINETT Sigma2, Grant No. NN9684K) are acknowledged for computer time.

Ethics statement

This work does not require any ethical statement.

Appendix A. Supplementary data

Optimized coordinates of the DFT calculations. Supplementary data to this article can be found online at <https://doi.org/10.1016/j.chem.2022.100332>.

References

- [1] S.B. Wu, C. Long, E.J. Kennelly, Structural diversity and bioactivities of natural benzophenones, *Nat. Prod. Rep.* 31 (2014) 1158–1174, <https://doi.org/10.1039/c4np00027g>.
- [2] M.S. Akhtar, R.S. Thombal, R.J. Inductivo Tamargo, W.G. Yang, S.H. Kim, Y.R. Lee, Eco-friendly organocatalyst- And reagent-controlled selective construction of diverse and multifunctionalized 2-hydroxybenzophenone frameworks for potent UV-A/B filters by cascade benzannulation, *Green Chem.* 22 (2020) 4523–4531, <https://doi.org/10.1039/d0gc01011a>.
- [3] D. Janssen-Müller, S. Singha, F. Lied, K. Gottschalk, F. Glorius, NHC-Organocatalyzed CAr–O Bond Cleavage: Mild Access to 2-Hydroxybenzophenones, *Angew. Chemie - Int. Ed.* 56 (2017) 6276–6279, <https://doi.org/10.1002/anie.201610203>.
- [4] J.M. Grandner, R.A. Cacho, Y.i. Tang, K.N. Houk, Mechanism of the P450-catalyzed oxidative cyclization in the biosynthesis of griseofulvin, *ACS Catal.* 6 (7) (2016) 4506–4511, <https://doi.org/10.1021/acscatal.6b01068>.
- [5] L. Saidi, D.H.A. Rocha, O. Talhi, Y. Bentarzi, B. Nedjar-Kolli, K. Bachari, F. A. Almeida Paz, L.A. Helguero, A.M.S. Silva, Synthesis of benzophenones and in vitro evaluation of their anticancer potential in breast and prostate cancer cells, *ChemMedChem* (2019), <https://doi.org/10.1002/cmdc.201900127>.
- [6] A.J. Szwalbe, K. Williams, Z. Song, K. De Mattos-Shipley, J.L. Vincent, A.M. Bailey, C.L. Willis, R.J. Cox, T.J. Simpson, Characterisation of the biosynthetic pathway to

- agnestins A and B reveals the reductive route to chrysophanol in fungi, *Chem. Sci.* 10 (2019) 233–238, <https://doi.org/10.1039/C8SC03778G>.
- [7] X.D. Ma, X. Zhang, S.Q. Yang, H.F. Dai, L.M. Yang, S.X. Gu, Y.T. Zheng, Q.Q. He, F. E. Chen, Synthesis and biological evaluation of (±)-benzhydryl derivatives as potent non-nucleoside HIV-1 reverse transcriptase inhibitors, *Bioorgan. Med. Chem.* 19 (2011) 4704–4709, <https://doi.org/10.1016/j.bmc.2011.07.003>.
- [8] S.K. Vooturi, C.M. Cheung, M.J. Rybak, S.M. Firestine, Design, synthesis, and structure – Activity relationships of benzophenone-based tetraamides as novel antibacterial agents, *J. Med. Chem.* 52 (2009) 5020–5031, <https://doi.org/10.1021/jm900519b>.
- [9] S.A. Khanum, S. Shashikanth, A.V. Deepak, Synthesis and anti-inflammatory activity of benzophenone analogues, *Bioorg. Chem.* 32 (2004) 211–222, <https://doi.org/10.1016/j.bioorg.2004.04.003>.
- [10] T. Tzanova, M. Gerova, O. Petrov, M. Karaivanova, D. Bagrel, Synthesis and antioxidant potential of novel synthetic benzophenone analogues, *Eur. J. Med. Chem.* 44 (2009) 2724–2730, <https://doi.org/10.1016/j.ejmech.2008.09.010>.
- [11] Y. Hayashi, H. Takeno, T. Chinen, K. Murguruma, K. Okuyama, A. Taguchi, K. Takayama, F. Yakushiji, M. Miura, T. Usui, Y. Hayashi, Development of a new benzophenone-diketopiperazine-type potent antimicrotubule agent possessing a 2-pyridine structure, *ACS Med. Chem. Lett.* 5 (2014) 1094–1098, <https://doi.org/10.1021/ml5001883>.
- [12] A. Guerrero-Corella, F. Esteban, M. Iniesta, A. Martín-Somer, M. Parra, S. Díaz-Tendero, A. Fraile, J. Alemán, 2-hydroxybenzophenone as a chemical auxiliary for the activation of ketiminoesters for highly enantioselective addition to alkenes under bifunctional catalysis, *Angew. Chemie Int. Ed.* 57 (2018) 5350–5354, <https://doi.org/10.1002/anie.201800435>.
- [13] A. Lee, H. Kim, Rhodium-catalyzed asymmetric 1,4-addition of α , β -unsaturated imino esters using chiral bicyclic bridgehead phosphoramidite ligands, *J. Am. Chem. Soc.* 137 (2015) 11250–11253, <https://doi.org/10.1021/jacs.5b07034>.
- [14] M.S. Seo, K. Kim, H. Kim, Controlling helical chirality of cobalt complexes by chirality transfer from vicinal diamines, *Chem. Commun.* 49 (2013) 11623–11625, <https://doi.org/10.1039/c3cc46887a>.
- [15] K. Ruhland, A. Obenhuber, S.D. Hoffmann, Cleavage of unstrained C(sp²)–C(sp²) single bonds with Ni⁰ complexes using chelating assistance, *Organometallics* 27 (2008) 3482–3495, <https://doi.org/10.1021/om800054m>.
- [16] E.E. Nekongo, P. Bagchi, C.J. Fahrmi, V.V. Popik, 9-Aryl-9-xanthenols: a convenient platform for the design of fluorimetric and colorimetric pH indicators, *Org. Biomol. Chem.* 10 (2012) 9214–9218, <https://doi.org/10.1039/c2ob26715b>.
- [17] M. Lalia-Kantouri, T. Dimitriadis, C.D. Papadopoulos, M. Gdaniec, A. Czapiak, A. G. Hatzidimitriou, Synthesis and structural characterization of iron(III) complexes with 2-hydroxyphenones, *Z. Anorg. Allg. Chem.* 635 (2009) 2185–2190, <https://doi.org/10.1002/zaac.200900016>.
- [18] M. Lalia-Kantouri, M. Gdaniec, C.D. Papadopoulos, K. Parinos, K. Chrissafis, B. Wicher, Correlation between structure and thermal properties in 2-hydroxybenzophenone Co(II) complexes, *J. Therm. Anal. Calorim.* 117 (3) (2014) 1241–1252, <https://doi.org/10.1007/s10973-014-3930-0>.
- [19] E. Mrkalić, A. Zianna, G. Psomas, M. Gdaniec, A. Czapiak, E. Coutouli-Argyropoulou, M. Lalia-Kantouri, Synthesis, characterization, thermal and DNA-binding properties of new zinc complexes with 2-hydroxyphenones, *J. Inorg. Biochem.* 134 (2014) 66–75, <https://doi.org/10.1016/j.jinorgbio.2014.01.019>.
- [20] A.A. Adeniyi, T.L. Ngake, J. Conradie, Cyclic Voltammetric Study of 2-hydroxybenzophenone (HBP) derivatives and the correspondent change in the orbital energy levels in different solvents, *Electroanalysis* 32 (12) (2020) 2659–2668, <https://doi.org/10.1002/elan.202060163>.
- [21] E. Chiyindiko, J. Conradie, An electrochemical and computational chemistry study of substituted benzophenones, *Electrochim. Acta* 373 (2021), 137894, <https://doi.org/10.1016/j.electacta.2021.137894>.
- [22] A.A. Adeniyi, J. Conradie, Exploring substituents and solvent effects on the reduction potential and molecular properties of five derivatives of hydroxybenzophenone (HBP) with their possible conformations and isomers, *Struct. Chem.* 32 (2021) 1299–1310, <https://doi.org/10.1007/s11224-020-01685-8>.
- [23] G. Gritzner, J. Kuta, Recommendations on reporting electrode potentials in nonaqueous solvents (Recommendations 1983), *Pure Appl. Chem.* 56 (1984) 461–466. doi:10.1351/pac198456040461.
- [24] A.D. Becke, Density-functional exchange-energy approximation with correct asymptotic behavior, *Phys. Rev. A* 38 (1988) 3098–3100, <https://doi.org/10.1103/PhysRevA.38.3098>.
- [25] C. Lee, W. Yang, R.G. Parr, Development of the Colle-Salvetti correlation-energy formula into a functional of the electron density, *Phys. Rev. B* 37 (1988) 785–789, <https://doi.org/10.1103/PhysRevB.37.785>.
- [26] [26] M.J. Frisch, G.W. Trucks, H.B. Schlegel, G.E. Scuseria, M.A. Robb, J.R. Cheeseman, G. Scalmani, V. Barone, G.A. Petersson, H. Nakatsuji, X. Li, M. Caricato, A. V. Marenich, J. Bloino, B.G. Janesko, R. Gomperts, B. Mennucci, H.P. Hratchian, J. V. Ortiz, A.F. Izmaylov, J.L. Sonnenberg, D. Williams-Young, F. Ding, F. Lipparini, F. Egidi, J. Goings, B. Peng, A. Petrone, T. Henderson, D. Ranasinghe, V.G. Zakrzewski, J. Gao, N. Rega, G. Zheng, W. Liang, M. Hada, M. Ehara, K. Toyota, R. Fukuda, J. Hasegawa, M. Ishida, T. Nakajima, Y. Honda, O. Kitao, H. Nakai, T. Vreven, K. Throssell, J. Montgomery, J. A., J.E. Peralta, F. Ogliaro, M.J. Bearpark, J.J. Heyd, E.N. Brothers, K.N. Kudin, V.N. Staroverov, T.A. Keith, R. Kobayashi, J. Normand, K. Raghavachari, A.P. Rendell, J.C. Burant, S.S. Iyengar, J. Tomasi, M. Cossi, J.M. Millam, M. Klene, C. Adamo, R. Cammi, J.W. Ochterski, R.L. Martin, K. Morokuma, O. Farkas, J.B. Foresman, D.J. Fox, *Gaussian 16*, Revision B.01, (2016).
- [27] A.V. Marenich, C.J. Cramer, D.G. Truhlar, Universal solvation model based on solute electron density and on a continuum model of the solvent defined by the bulk dielectric constant and atomic surface tensions, *J. Phys. Chem. B* 113 (2009) 6378–6396, <https://doi.org/10.1021/jp810292n>.
- [28] R.E. Skynner, J.L. McDonagh, C.R. Groom, T. van Mourik, J.B.O. Mitchell, A review of methods for the calculation of solution free energies and the modelling of systems in solution, *Phys. Chem. Chem. Phys.* 17 (9) (2015) 6174–6191, <https://doi.org/10.1039/c5cp00288e>.
- [29] Chemcraft - graphical software for visualization of quantum chemistry computations., (n.d.). <http://www.chemcraftprog.com/>.
- [30] R.S. Mulliken, A new electroaffinity scale; Together with data on valence states and on valence ionization potentials and electron affinities, *J. Chem. Phys.* 2 (1934) 782–793, <https://doi.org/10.1063/1.1749394>.
- [31] M.V. Putz, N. Russo, E. Sicilia, About the Mulliken electronegativity in DFT, *Theor. Chem. Acc.* 114 (2005) 38–45, <https://doi.org/10.1007/s00214-005-0641-4>.
- [32] F. De Proft, W. Langenaeker, P. Geerlings, Ab initio determination of substituent constants in a density functional theory formalism: calculation of intrinsic group electronegativity, hardness, and softness, *J. Phys. Chem.* 97 (1993) 1826–1831, <https://doi.org/10.1021/j100111a018>.
- [33] R.G. Parr, L.V. Szentpály, S. Liu, Electrophilicity index, *J. Am. Chem. Soc.* 121 (1999) 1922–1924, <https://doi.org/10.1021/ja983494x>.
- [34] R.G. Pearson, Physical Hardness, in: *Chem. Hardness*, Wiley-VCH Verlag GmbH & Co. KGaA, Weinheim, FRG, 2005: pp. 175–195. doi:10.1002/3527606173.ch6.
- [35] R.G. Parr, R.G. Pearson, Absolute hardness: companion parameter to absolute electronegativity, *J. Am. Chem. Soc.* 105 (1983) 7512–7516, <https://doi.org/10.1021/ja00364a005>.
- [36] R.G. Parr, R.A. Donnelly, M. Levy, W.E. Palke, Electronegativity: the density functional viewpoint, *J. Chem. Phys.* 68 (1978) 3801–3807, <https://doi.org/10.1063/1.436185>.
- [37] W. Yang, R.G. Parr, Hardness, softness, and the Fukui function in the electronic theory of metals and catalysis, *Proc. Natl. Acad. Sci. U. S. A.* 82 (1985) 6723–6726, <https://doi.org/10.1073/pnas.82.20.6723>.
- [38] S.R. Gadre, R.N. Shirsat, *Electrostatics of Atoms and Molecules*, Universities Press, India, 2001.
- [39] A.A. Adeniyi, M. Landman, J. Conradie, Mo Fischer carbene complexes: a DFT study on the prediction of redox potentials, *J. Electrochem. Soc.* 168 (6) (2021) 066523, <https://doi.org/10.1149/1945-7111/ac0a28>.
- [40] J. Grimshaw, R. Hamilton, Steric and electronic effects on the redox potentials of benzophenone radical anions, *J. Electroanal. Chem. Interfacial Electrochem.* 106 (1980) 339–346, [https://doi.org/10.1016/S0022-0728\(80\)80179-3](https://doi.org/10.1016/S0022-0728(80)80179-3).
- [41] C. Hansch, A. Leo, R.W. Taft, A survey of Hammett substituent constants and resonance and field parameters, *Chem. Rev.* 91 (1991) 165–195, <https://doi.org/10.1021/cr00002a004>.
- [42] M. Charton, The application of the Hammett equation to ortho-substituted benzene reaction series I, *Can. J. Chem.* 38 (1960) 2403–2499, <https://doi.org/10.1139/v60338>.
- [43] N. Elgrishi, K.J. Rountree, B.D. McCarthy, E.S. Rountree, T.T. Eisenhart, J. L. Dempsey, A practical beginner's guide to cyclic voltammetry, *J. Chem. Educ.* 95 (2018) 197–206, <https://doi.org/10.1021/acs.jchemed.7b00361>.
- [44] P.T. Kissinger, W.R. Heineman, Cyclic voltammetry, *J. Chem. Educ.* 60 (1983) 702–706, <https://doi.org/10.1021/ed060p702>.
- [45] R.L. Birke, M. Kim, M. Strassfeld, Diagnosis of reversible, quasi-reversible, and irreversible electrode processes with differential pulse polarography, *Anal. Chem.* 53 (1981) 852–856, <https://doi.org/10.1021/ac00229a026>.
- [46] M.V. Mirkin, A.J. Bard, Simple analysis of quasi-reversible steady-state voltammograms, *Anal. Chem.* 64 (1992) 2293–2302, <https://doi.org/10.1021/ac00043a020>.
- [47] J.C. Myland, K.B. Oldham, Quasireversible cyclic voltammetry of a surface confined redox system: a mathematical treatment, *Electrochem. Commun.* 7 (2005) 282–287, <https://doi.org/10.1016/j.elecom.2005.01.005>.
- [48] R. Freitag, J. Conradie, Electrochemical and computational chemistry study of Mn(β -diketonato)3 complexes, *Electrochim. Acta* 158 (2015) 418–426, <https://doi.org/10.1016/j.electacta.2015.01.147>.
- [49] M.M. Conradie, J. Conradie, Electrochemical behaviour of Tris(β -diketonato)iron(III) complexes: a DFT and experimental study, *Electrochim. Acta* 152 (2015) 512–519, <https://doi.org/10.1016/j.electacta.2014.11.128>.
- [50] M. Landman, R. Pretorius, R. Fraser, B.E. Buitendach, M.M. Conradie, P.H. van Rooyen, J. Conradie, Electrochemical behaviour and structure of novel phosphine- and phosphite-substituted tungsten(0) Fischer carbene complexes, *Electrochim. Acta* 130 (2014) 104–118, <https://doi.org/10.1016/j.electacta.2014.02.127>.
- [51] R. Liu, J. Conradie, Tris(β -diketonato)chromium(III) complexes: effect of the β -diketonate ligand on the redox properties, *Electrochim. Acta* 185 (2015) 288–296, <https://doi.org/10.1016/j.electacta.2015.10.116>.
- [52] A. Kuhn, J. Conradie, Electrochemical and density functional theory study of bis(cyclopentadienyl) mono(β -diketonato) titanium(IV) cationic complexes, *Electrochim. Acta* 56 (2010) 257–264, <https://doi.org/10.1016/j.electacta.2010.08.086>.
- [53] P.K. Chattaraj, U. Sarkar, D.R. Roy, Electrophilicity index, *Chem. Rev.* 106 (2006) 2065–2091, <https://doi.org/10.1021/cr040109f>.
- [54] B.A. Anjali, F.B. Sayyed, C.H. Suresh, Correlation and prediction of redox potentials of hydrogen evolution mononuclear cobalt catalysts via molecular electrostatic potential: a DFT study, *J. Phys. Chem. A* 120 (2016) 1112–1119, <https://doi.org/10.1021/acs.jpca.5b11543>.
- [55] B.A. Anjali, C.H. Suresh, Electronic effect of ligands vs. reduction potentials of Fischer carbene complexes of chromium: a molecular electrostatic potential analysis, *New J. Chem.* 42 (2018) 18217–18224, <https://doi.org/10.1039/C8NJ04184A>.